Superconductor Science and Technology

PAPER • **OPEN ACCESS**

A dual-band cold-electron bolometer with on-chip filters for the 220/240 GHz channels of the LSPE instrument

To cite this article: L S Kuzmin *et al* 2019 *Supercond. Sci. Technol.* **32** 084005

OPEN ACCESS
IOP Publishing
Superconductor Science and Technology
Supercond. Sci. Technol. **32** (2019) 084005 (6pp)
https://doi.org/10.1088/1361-6668/ab214b

A dual-band cold-electron bolometer with on-chip filters for the 220/240 GHz channels of the LSPE instrument

L S Kuzmin[1,2], D A Pimanov[2], A V Gordeeva[2,3], A V Chiginev[2,3], S Masi[4] and P de Bernardis[4]

[1] Chalmers University of Technology, Gothenburg SE-41296, Sweden
[2] Nizhny Novgorod State Technical University n. a. R. E. Alekseev, Nizhny Novgorod 603951, Russia
[3] Institute for Physics of Microstructures, Russian Academy of Sciences, Nizhny Novgorod, 603950, Russia
[4] Dipartimento di Fisica, Universit'a La Sapienza, P. le A. Moro 2, I-00185 Roma, Italy

E-mail: kuzmin@chalmers.se

Received 30 November 2018, revised 21 April 2019
Accepted for publication 13 May 2019
Published 1 July 2019

Abstract

We are developing multi-chroic double-slot antenna with cold-electron Bolometer (CEB) on-chip filters for the 220/240 GHz interstellar dust monitoring channels of the LSPE–SWIPE experiment. For this goal, we used a narrowband double-slot resonant antenna with CEBs connected by coplanar lines. The simulations show that we have achieved 5% bandwidth for 220 GHz and 5.5% bandwidth for 240 GHz in our numeric modeling for the single cells. A series array of unit cells using double-slot design and coplanar lines with CEBs shows proper frequency selection. Estimations of the noise properties of the CEB arrays in a voltage-biased mode with the SQUID readout show photon-noise limited operation for the optical power load of 6 pW for channel 220 GHz and 20 pW for channel 240 GHz.

Keywords: SQUID, cold-electron bolometer, double-slot antenna, dual-band, SIN tunnel junction

(Some figures may appear in colour only in the online journal)

1. Introduction

The Large-Scale Polarization Explorer (LSPE) [1] is an experiment with two instruments to measure the B-mode polarization pattern of the cosmic microwave background (CMB). This observable provides a unique way to study ultra-high-energy physics phenomena, like cosmic inflation, happening the first split-second after the big bang. To date, only upper limits exist for the inflation-related contribution to the B-mode polarization of the CMB, specified by a tensor to scalar ratio (between the tensor fluctuations and the scalar ones) $r < 0.07$. The main difficulty of these measurements nowadays is the control of the contribution from the polarized emission of the interstellar medium in our Galaxy (synchrotron emission at low frequencies, dust emission at high frequencies). At frequencies close to the maximum of the specific brightness of the CMB (150 GHz), the polarized emission from interstellar dust represents a severe contamination (see e.g. [2]) and must be measured with sub-% accuracy to allow for a reliable estimate of the B-modes from inflation at levels of the order of $r = 0.01$. To this purpose, multi-frequency polarimeters have been developed, covering a frequency range wide enough to monitor accurately the polarized emission from dust. Its specific brightness rises fast with frequency, and at 350 GHz is dominant. However, the spectral shape of interstellar dust emission is variable across the sky, due to the presence of a different number of dust clouds—with different temperature, optical depth and possibly composition—along different lines of sight. This means that a simple linear scaling of a high frequency monitoring channel could be insufficient to estimate the contribution of

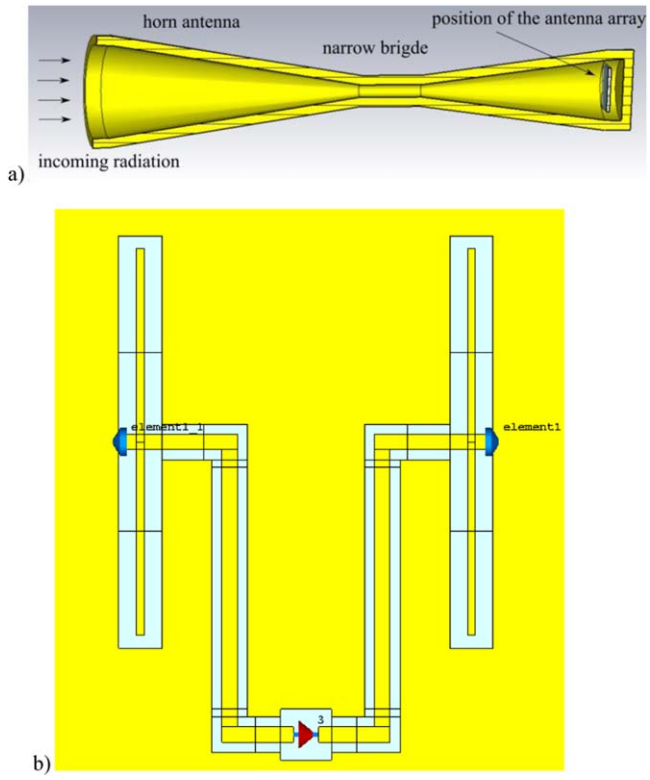

Figure 1. (a) A schematic view of the back-to-back feedhorn, (b) Single cell of double-slot antenna design overview in CST Microwave Studio.

dust in the CMB channel. In LSPE it was decided to use two dust monitoring channels, as close as possible to the CMB frequency, so that the extrapolation is less affected by uncertainties in the knowledge of the dust spectrum.

The short wavelength instrument for the polarization explorer (SWIPE) is aimed at a measurement of B-modes with a final uncertainty on r of 0.01 (at 68% C. L.), thanks to an internal ability to remove dust polarization, in synergy with the other instrument of LSPE (STRIP) which allows removal of the polarized synchrotron contribution.

LSPE–SWIPE is a balloon-borne polarimeter, mapping a large fraction (>25%) of the sky, with coarse angular resolution (1° FWHM) at 150, 220, 240 GHz. The 150 GHz band (20% wide) has been selected to provide high sensitivity to CMB polarization fluctuations, while the 220 and 240 GHz bands (5% wide) provide sensitive monitoring of the polarized brightness of interstellar dust. The instrument design traded angular resolution for sensitivity, using multi-moded back-to-back feedhorns in the focal plane to illuminate multi-moded detectors (for a total of 330 pixels). Polarization sensitivity is obtained by means of a cryogenic rotating HWP.

The baseline detectors for SWIPE are TES bolometers, complemented by quasi-optical filters providing frequency band selection [3]. Here we study an alternative approach, based on on-chip filters and cold-electron bolometers [4–7]. In this alternative design, a planar array of CEBs and slot antennas is placed at the exit of the feedhorn (figure 1(a)), so that the radiation diagrams of the slot themselves will not affect the beam characteristics of the receiver. The use of a dual-band detector within a single feedhorn provides a non-negligible instrument sensitivity advantage with respect to the baseline (where each feedhorn feeds only a single-frequency detector) keeping a fixed size of the focal plane and a fixed number of feedhorns. With respect to the current baseline (110 antennas with 110 detectors for each band) the focal plane layout could be maintained, assigning 220 antennas with single detectors to the 150 GHz band, and 110 antennas with dual band detectors to the 220/240 GHz bands. This would result in a 40% improvement of the sensitivity of the CMB channel, maintaining the same sensitivity for the dust monitoring channels.

2. Single cell for the double-slot antenna with folded coplanar lines and CEBs

The requirement to create on-chip filters with a bandwidth of 5% is not trivial task. First of all we tested a natural idea to use capacitance of the SIN tunnel junction and a kinetic inductance of NBN strip [8, 9]. However, for this structure inserted in a cross-slot antenna gave wide bandwidth at the level of 10% and more. The next step was testing a seashell antenna double-slot antennas and microstrip lines feeded near the ends of the slots [10, 11]. However, this structure again gave relatively high bandwidth. Besides, many parasitic resonances were organized in this nonsymmetric structure.

The decisive step was to use double slot antenna with feeding from the center (the place with high impedance) by coplanar lines (CPW) to low ohmic CEB. The CPW serves as transformer between these impedances. Using narrowband resonance of slots and CPW we managed to get required 5% bandwidth of the system.

The design of a single cell of a Double-Slot antenna is shown in figure 1(a). The antenna consists of 2 resonant slots and folded coplanar lines. The length of the coplanar lines was chosen to get the required operating frequency. The distance between slots was chosen due to test simulations in CST Microwave Studio to get the required bandwidth. CEB is put into the gap in the central wire of the coplanar. The position of CEB is indicated by red triangle in figure 1(b).

The DC biasing of CEB is provided through coplanar lines by DC connectors, which are set under the ground plane. The positions of DC connectors are indicated by blue triangles in figure 1(b). In the numerical modelling, the influence of the DC connectors on the antenna electrodynamics is taken into account. The DC connectors are simulated by the lumped capacitances, which are connected between coplanar lines and ground plane. These lumped elements are set to 350 fF, it is the calculated value of DC connectors capacitance.

Figure 1(b) shows the single cell for antenna for 220 GHz. There is only one difference in antenna design in case of 240 GHz, the total length of central coplanar line; it is 60 um shorter to get 240 GHz. In Frequency Domain Solver of CST Microwave Studio, these designs have the results shown in figures 2(a) and (b). These calculations have been run in electrodynamics.

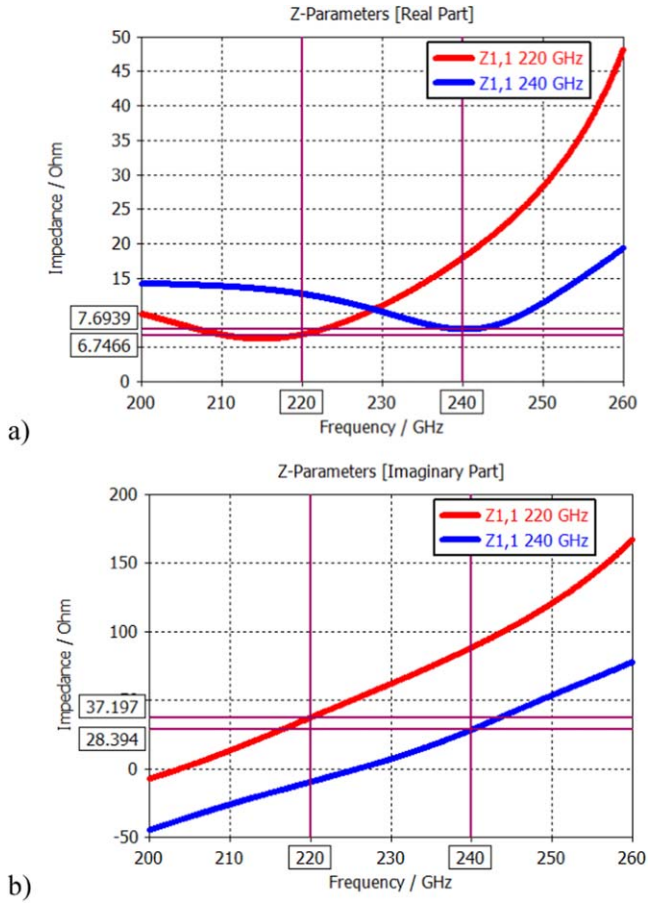

Figure 2. (a) ReZ and (b) ImZ for 220 GHz (red) and 240 GHz (blue) Double-Slot antennas.

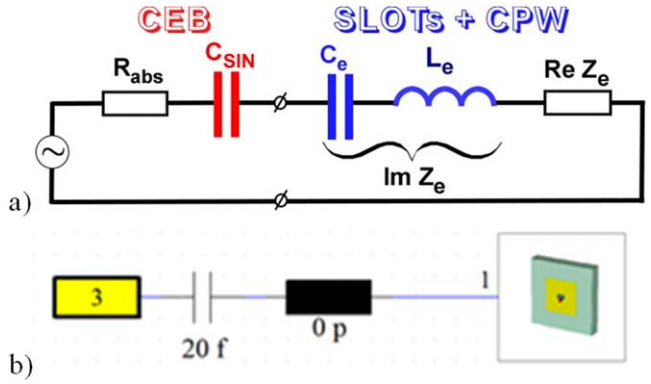

Figure 3. (a) Equivalent circuit of the Double-Slot antenna connected with a CEB; (b) the equivalent circuit used in the numerical modeling.

From figure 2(a) one can see, that ReZ minimums are around 220 GHz for red line and 240 GHz for blue line. Figure 2(b) shows that ImZ curves go almost parallel.

Here ReZ (220 GHz) is 6.8 Ohm, ReZ (240 GHz) is 7.7 Ohm; ImZ (220 GHz) is 36.3 Ohm, ImZ (240 GHz) is 32.9 Ohm. These values are important for further obtaining the required resonances at needed operating frequencies in schematics.

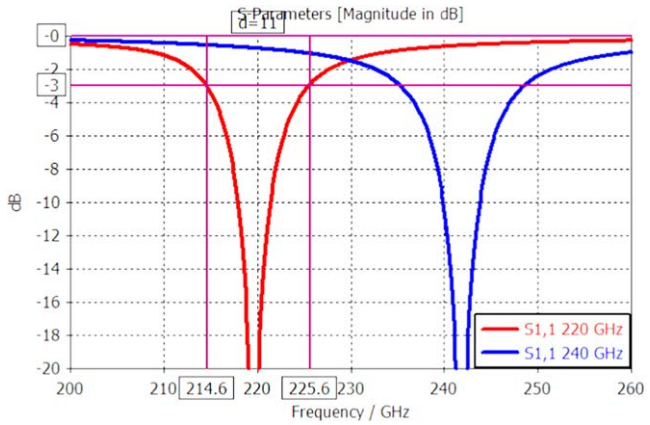

Figure 4. Frequency characteristics of Double-Slot antennas with CEBs tuned to 220 GHz (red) and 240 GHz (blue) in CST MWS schematic.

The equivalent circuit of the double-slot antenna connected with a CEB is shown on figure 3(a), and its simulation model is presented on figure 3(b). Here the values of R_{abs} and C_{SIN} are chosen in the following way: $R_{abs} = \mathrm{Re}Z(f_0)$, $C_{SIN} = (2\pi f_0 \cdot \mathrm{Im}Z(f_0))^{-1}$, where $Z(f)$ is the diagonal component of the Z-matrix calculated in electrodynamics (see above). Here C_{SIN} values are chosen to make the total capacitances of C_{SIN} and C_e form the series resonance with L_e at operating frequencies 220 and 240 GHz respectively. This way of schematic parameters choice is valid only when $\mathrm{Im}Z(f_0) > 0$ and when $|S_{mn}(f_0)| \ll 1$, where S_{mn} are the non-diagonal components of the S-parameters matrix which is calculated in electrodynamics.

Figure 4 shows the frequency characteristics after using the results from electrodynamics calculation in schematic part. For 220 GHz antenna, R_{abs} is 6.8 Ohm, and for 240 GHz antenna, R_{abs} is 7.7 Ohm. C_{SIN} for both frequencies is 20 fF, it hits the fabrication technology restriction. These values are set to obtain the best impedance matching at operating frequencies.

As we can see on figure 4, the widths of resonances are nearly 11 GHz and 13 GHz for operating frequencies 220 and 240 GHz respectively. Bandwidth for 220 GHz meets the requirements for the receiving system of LSPE experiment; it is 5% from operating frequency. Bandwidth for 240 GHz is close to meet the requirements for the receiving system of LSPE experiment; it is 5.5% from operating frequency.

3. An array of multi-chroic double-slot antennas with coplanar lines and CEBs

For matching the CEB with high optical power load we use a concept of 2D array of bolometers distributed over Airy spot [5, 12]. Here we consider an array of slot antennas which are connected in series by coplanar waveguides (CPW). The main advantage of this approach is a simple one-layer technology, which implies that the DC connections between CEBs are made by the same CPWs that connect the antennas in AC. This solution greatly simplifies the technology. For the

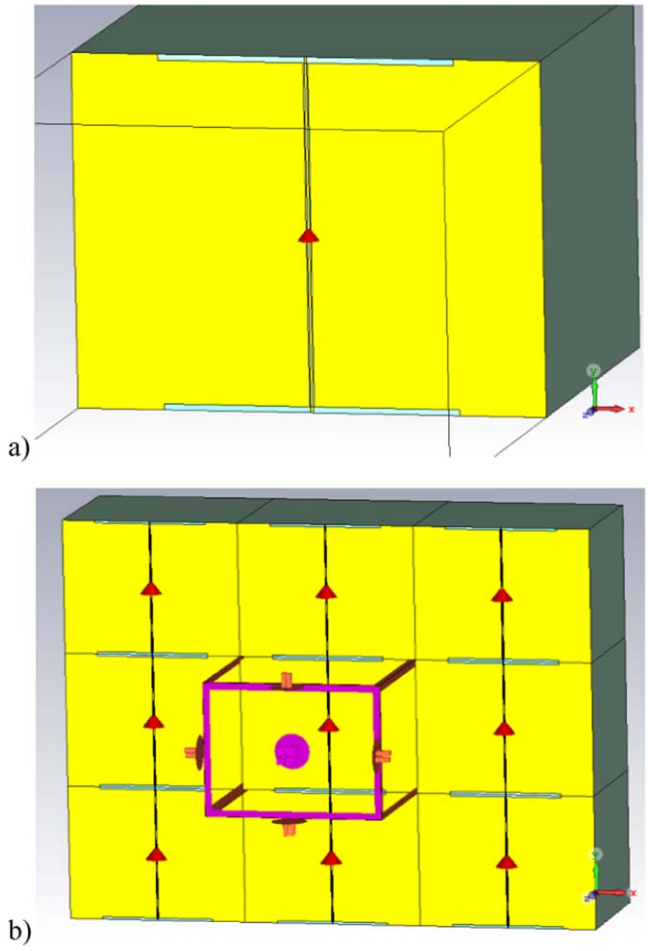

Figure 5. (a) One unit cell of the entire slot antenna array; (b) a part of the entire array.

current state, this solution is easier to use for the array current-biased CEBs.

To model the antenna system with slots, we use the following approach. First, we perform calculations of one unit cell of the entire slot antenna array (figure 5(a)). The unit cell consists of a ground plane (shown by yellow), two halves of the slot antenna, which are located in upper and lower parts of the cell, and the coplanar line, which connects these slot halves. The CEB is inserted into the gap in the middle of the coplanar line. The boundary conditions at $X_{\min}$, $X_{\max}$ and $Y_{\min}$, $Y_{\max}$ are periodic, thus making the entire system infinite in X and Y directions (figure 5(b)).

The calculations have been made in CST Microwave Studio. We use frequency domain to model the frequency characteristics of the unit cell. We calculate S-parameters of the unit cell in electrodynamics, and then obtain Z-parameters by post-processing. To model CEB, we use RC chain, where R is the absorber resistance; C is the capacitance of two series SIN junctions of the CEB. Using Z-parameters, we find the values of R_{abs} and C_{SIN}, by relations $C_{\text{SIN}} = (2\pi f_0 \cdot \text{Im}Z(f_0))^{-1}$, $R_{\text{abs}} = \text{Re}Z(f_0)$. These relations provide resonance at operating frequency f_0. The final schematics result is shown in figure 6(a). Figure 6(b) shows the resonance at 220 GHz in the S-parameter of the antenna unit

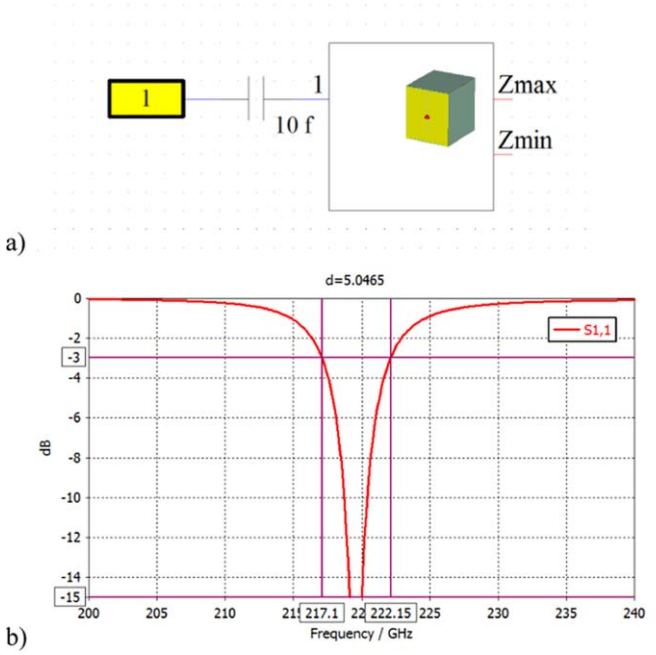

Figure 6. (a) The equivalent circuit of the CEB connected to the unit cell of the antenna array; (b) S-parameter of the unit cell of the antenna with CEB.

cell. We see that the resonance is very sharp with the width of 5 GHz, and well meets the requirement of 5% of operating frequency made to the resonance. There are also two parasitic resonances in S-parameter curve (figure 6(b), not visible).

Next, we use the obtained values of R and C to model the more real situation, specifically, the finite array of the slot antennas connected by the coplanar lines. The appearance of this array is shown in figure 7. It is seen that the $3 \times 3\ \text{mm}^2$ substrate contains 45 slots for 220 GHz channel and 45 slots for 240 GHz channel. Here the dimensions of all parts of the unit cell for 240 GHz channel are obtained from those of 220 GHz channel cell by scaling. On the back side of the ground plane there is a waveguide port which we use as a source of the electromagnetic radiation. In the present calculations we restrict ourselves to the case of mode E_{01}.

Figure 8 shows the power accepted by all absorbers of the CEB in one frequency channel. Two kinds of curves are presented—for 36 and 45 slots per channel. We see that the curves have resonant shape, and the maxima of the resonances are nearly at 220 and 240 GHz respectively. As expected, the maxima for 45 slots per channel are higher than those for 36 slots per channel.

Table 1 shows widths of the resonant curves for 220 and 240 GHz frequency channels. We see that widths of the resonances only slightly exceed the requirements of 5% of operating frequency.

4. Matching of cold-electron bolometers with SQUID read-out

The multiplexing becomes an essential part of the read-out systems, since it reduces the cost and simplifies the

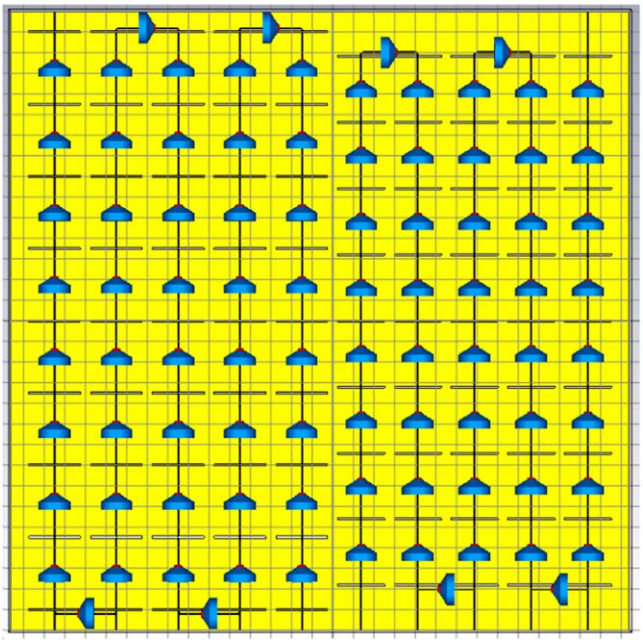

Figure 7. The finite array of slot antennas consisting of 45 slots for 220 GHz channel (left part) and 45 slots for 240 GHz channel (right part). The blue and red triangles denote capacitance and absorber resistance of CEB, respectively. The size of the substrate is 3×3 mm^2.

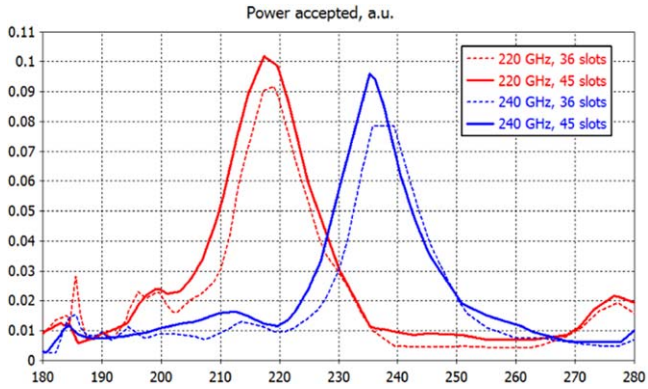

Figure 8. Power accepted by all CEBs' absorbers, versus frequency.

Table 1. Widths of the resonant curves in figure 8.

	FWHM, 220 GHz channel		FWHM, 240 GHz channel	
	GHz	%	GHz	%
36 slots	14	6.4	14.2	5.9
45 slots	16.9	7.7	14.2	5.9

implementation, especially for large arrays of pixels. The multiplexing, developed for TES bolometers, goes together with SQUID read-out [13]. SQUID read-out system is known as a low noise read-out. That is why it is widely used, for example, with TES bolometers. Here we check the possibility to use such read-out for cold electron bolometers.

Usually SQUIDs are used with sensors, which typical resistance is of the order of several Ohms or less. The

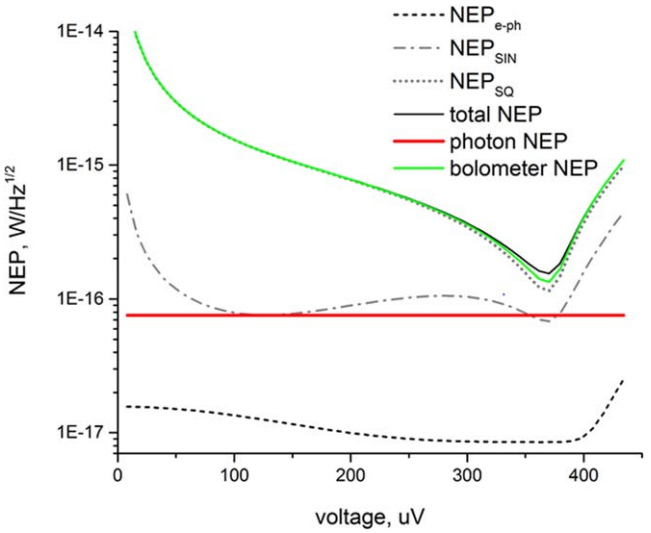

Figure 9. NEP versus voltage of an array from 20 bolometers, connected in parallel, with SQUID read-out for 220 GHz channel.

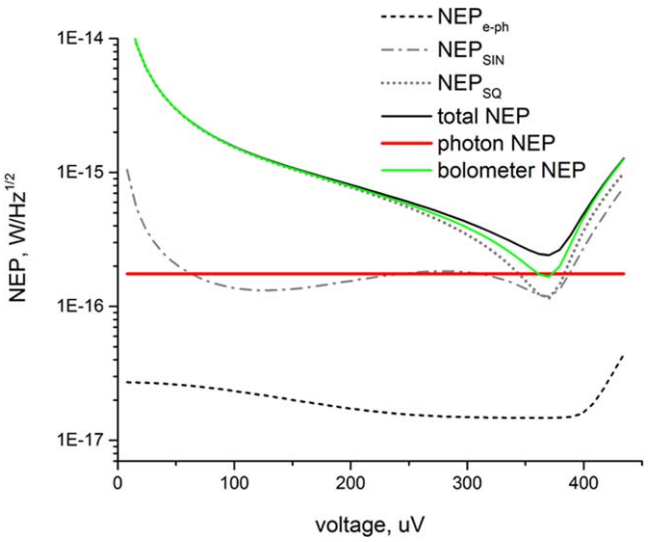

Figure 10. NEP versus voltage of an array from 60 bolometers, connected in parallel, with SQUID read-out for 240 GHz channel.

resistance of a single cold electron bolometer in operation point in voltage bias mode is of the order of several hundred Ohm. In order to reduce the impedance, several CEBs can be connected in parallel. Let us estimate the noise equivalent power (NEP) of parallel CEB array for SQUID read-out. The SQUID array sensitivity is 3.5 pA Hz$^{-1/2}$.

The optical power load for channel 220 GHz is 6 pW, and for channel 240 GHz–20 pW. For estimation of NEP we used a heat-balance equation method for array of CEBs [14]. Considering that one CEB can receive up to 0.3 pW, the channel 220 requires at least 20 bolometers, and channel 240–60 bolometers.

The noise equivalent power, calculated for 20 and 60 parallel connections of CEBs, is shown in figures 9 and 10. The normal resistance of one bolometer is 1 kOhm.

The photon NEP of the array for 220 GHz channel is 7.6×10^{-17} W Hz$^{-1/2}$. And the bolometer NEP is 1.4×10^{-16} W Hz$^{-1/2}$.

For 240 GHz channel, the results are following: the photon NEP is 1.8×10^{-16} W Hz$^{-1/2}$, and the bolometer NEP is 1.6×10^{-16} W Hz$^{-1/2}$. This relation means that the cold-electron bolometers are photon-noise-limited.

5. Conclusions

We have developed a proper design of single cell for a double-slot antenna with folded coplanar lines, connected to CEB, for fabrication. The single cell results for 220 GHz meet the frequency and bandwidth requirements for the LSPE project. The single cell results for 240 GHz slightly exceed the bandwidth requirements for the LSPE project. So this design will be further improved and used in array design too.

The simulations have been done also for the current-biased array of a various number of unit cells consisting of two slots with coplanar lines, connected to CEB. The unique feature of this design is that only one RF layer is used for the structure. The widths of resonances for this approach only slightly exceed the bandwidth requirements of 5% of operating frequencies. The minimal reached bandwidth at 220 GHz is 6.4%, at 240 GHz it is 5.9%. Further research will be aimed at improving these results to meet the LSPE project requirements.

Besides, some research was done for matching of CEBs with SQUID read-out where the possibility to use such read-out for cold electron bolometers is checked. Here we conclude that CEBs are photon noise limited detector for given power load.

Acknowledgments

The authors would like to thank L Lamagna, S Shitov, A Sobolev and A Pankratov for useful discussions. The work is supported by the Ministry of Education and Science of Russian Federation (Project 16.2562.2017/PCh).

ORCID iDs

L S Kuzmin https://orcid.org/0000-0002-8051-484X
A V Chiginev https://orcid.org/0000-0002-6676-9141

References

[1] LSPE collaboration, Aiola S. and et al. 2012 The large-scale polarization explorer (LSPE) *Proc. SPIE* **8446** 84467A
[2] Planck collaboration 2016 Planck intermediate results. XXX. The angular power spectrum of polarized dust emission at intermediate and high galactic latitudes *Astron. Astrophys.* **586** A133
[3] Gualtieri R *et al* 2016 *J. Low Temp. Phys.* **184** 527–33
[4] Kuzmin L 2002 *International Workshop On Superconducting Nano-Electronics Devices* ed J Pekola *et al* (Boston, MA: Springer) pp 145–54
Kuzmin L and Golubev D 2002 *Physica* C **372–376** 378
[5] Kuzmin L 2008 *J. Phys. Conf. Ser.* **97** 012310
[6] Tarasov M A, Kuzmin L S, Edelman V S, Mahashabde S and de Bernardis P 2011 *IEEE Trans. Appl. Supercond.* **21** 3635
[7] Salatino M, de Bernardis P, Kuzmin L S, Mahashabde S and Masi S 2014 *J. Low Temp. Phys.* **176** 323
[8] Kuzmin L S 2014 *IEEE Trans. Terahertz Sci. Technol.* **4** 314–20
[9] Kuzmin L S, Mukhin A S and Chiginev A V 2018 *IEEE Trans. Appl. Supercond.* **28** 2400304
[10] Kuzmin L S, Chiginev A V, Matrozova E A and Sobolev A S 2016 *IEEE Trans. Appl. Supercond.* **26** 2300206
[11] Kuzmin L S and Chiginev A V 2016 *Proc. SPIE* **9914** 99141U
[12] Kuzmin L S 2011 *Radiophys. Quantum Electron.* **54** 548–56
[13] Vaccaro D *et al* 2018 *Nucl. Instrum. Methods Phys. Res.* A (https://doi.org/10.1016/j.nima.2018.10.116)
[14] Gordeeva A V *et al* 2017 *Appl. Phys. Lett.* **110** 162603